

1 **Subglacial hydrological control on flow of an Antarctic Peninsula palaeo-ice stream**

2

3 Robert D. Larter<sup>1\*</sup>, Kelly A. Hogan<sup>1</sup>, Claus-Dieter Hillenbrand<sup>1</sup>, James A. Smith<sup>1</sup>, Christine L.  
4 Batchelor<sup>2</sup>, Matthieu Cartigny<sup>3</sup>, Alex J. Tate<sup>1</sup>, James D. Kirkham<sup>1,2</sup>, Zoë A. Roseby<sup>4,1</sup>, Gerhard Kuhn<sup>5</sup>,  
5 Alastair G.C. Graham<sup>6</sup>, and Julian A. Dowdeswell<sup>2</sup>

6

7 <sup>1</sup>British Antarctic Survey, Madingley Road, High Cross, Cambridge CB3 0ET, UK.

8 <sup>2</sup>Scott Polar Research Institute, University of Cambridge, Lensfield Road, Cambridge CB2 1ER, UK.

9 <sup>3</sup>Department of Geography, South Road, Durham University, Durham DH1 3LE, UK.

10 <sup>4</sup>Ocean and Earth Science, National Oceanography Centre, University of Southampton Waterfront  
11 Campus, European Way, Southampton SO14 3ZH, UK.

12 <sup>5</sup>Alfred Wegener Institute, Helmholtz-Centre for Polar and Marine Research, D-27568 Bremerhaven,  
13 Germany.

14 <sup>6</sup>College of Life and Environmental Sciences, University of Exeter, Rennes Drive, Exeter EX4 4RJ, UK

15 **Correspondence:** Robert D. Larter (rdla@bas.ac.uk).

16

17

18 **Abstract.** Basal hydrological systems play an important role in controlling the dynamic behaviour of  
19 ice streams. Data showing their morphology and relationship to geological substrates beneath  
20 modern ice streams are, however, sparse and difficult to collect. We present new multibeam  
21 bathymetry data that make the Anvers-Hugo Trough west of the Antarctic Peninsula the most  
22 completely surveyed palaeo-ice stream pathways in Antarctica. The data reveal a diverse range of  
23 landforms, including streamlined features where there was fast flow in the palaeo-ice stream,  
24 channels eroded by flow of subglacial water, and compelling evidence of palaeo-ice stream shear  
25 margin locations. We interpret landforms as indicating that subglacial water availability played an  
26 important role in facilitating ice stream flow and controlling shear margin positions. Water was likely  
27 supplied to the ice stream bed episodically as a result of outbursts from a subglacial lake located in  
28 the Palmer Deep basin on the inner continental shelf. These interpretations have implications for  
29 controls on the onset of fast ice flow, the dynamic behaviour of palaeo-ice streams on the Antarctic  
30 continental shelf, and potentially also for behaviour of modern ice streams.

31

32

## 33 1. Introduction

34

35 There is growing evidence that basal hydrology is a critical factor controlling the dynamic behaviour  
36 of ice streams (Bell, 2008; Christianson et al., 2014; Christoffersen et al., 2014), which account for  
37 most of the mass loss from large ice sheets. Understanding ice stream dynamics, including basal  
38 hydrology, is thus essential for quantifying ice sheet contributions to sea level change. Subglacial  
39 lakes and areas of elevated geothermal heat flux have been discovered in the onset regions of  
40 several large ice streams (Fahnestock et al., 2001; Bell et al., 2007; Stearns et al., 2008). Obtaining  
41 high resolution topographic data from modern ice stream beds that can reveal features associated  
42 with subglacial water flow is, however, logistically difficult and time consuming (e.g. Christianson et  
43 al., 2012). In contrast, modern ship-mounted sonar systems can be used to obtain such data  
44 efficiently over extensive areas of former ice stream beds on continental shelves that ice has  
45 retreated from since the Last Glacial Maximum (LGM; 23-19 k cal yr BP).

46 Knowledge and interpretations of submarine glacial landforms have advanced rapidly over the  
47 past two decades (Dowdeswell et al., 2016). For example, it is now recognised that elongated  
48 drumlins and mega-scale glacial lineations (MSGL) are signatures of past streaming ice flow on wet-  
49 based, mainly sedimentary beds, and that elongation generally increases with increasingly fast past  
50 flow rates (Stokes and Clark, 1999; Ó Cofaigh et al., 2002). The degree of preservation of fields of  
51 MSGL and the extent to which they are overprinted by grounding zone wedges and transverse  
52 moraines provides an indication to the rapidity of past grounding line retreat (Ó Cofaigh et al., 2008).  
53 'Hill-hole pairs' and sediment rafts are recognised as features formed by glaciotectonic processes  
54 beneath cold, dry based ice (Evans et al., 2006; Klages et al., 2015). Erosion of meandering or  
55 anastomosing seabed channels and tunnel valleys with reversals of gradient along their length  
56 requires a hydrological pressure gradient that indicates they could only have formed beneath  
57 grounded ice (Ó Cofaigh et al., 2002; Nitsche et al., 2013). Simple hydrological pressure calculations  
58 indicate that a gentle ice surface gradient produces a pressure gradient at the bed that will drive  
59 water up an opposing bed slope nearly ten times as steep.

60 Modern ice sheet observations have revealed increases in ice flow rates over timescales of days  
61 to years in response to Antarctic subglacial drainage events (Stearns et al., 2008; Siegfried et al.,  
62 2016). Responses of glaciers in southwest Greenland to seasonal drainage of supraglacial meltwater  
63 to the bed, however, show that the mode of subglacial drainage is important, as a slow-down of  
64 glacier flow above a certain run-off threshold has been interpreted to correspond to a switch to  
65 more efficient, channelized drainage (Sundal et al., 2011).

66 Here we present extensive new multibeam bathymetry data from the Anvers-Hugo Trough (AHT)  
67 west of the Antarctic Peninsula (Fig. 1). We interpret bedforms revealed by these data as evidence of  
68 a basal hydrological system that influenced the flow and lateral extent of the palaeo-ice stream and  
69 was fed by a subglacial lake in a deep basin on the inner continental shelf. We use heritage  
70 multichannel seismic (MCS) and deep tow boomer (DTB) data to constrain the nature of substrates  
71 beneath the LGM deposits and their potential influence on the basal hydrological system and  
72 sediment supply.

73

#### 74 **1.1 Glacial history and setting**

75

76 Drilling results and seismic reflection profiles indicate that the Antarctic Peninsula Ice Sheet has  
77 advanced to its western continental shelf edge many times since the late Miocene (Larter et al.,  
78 1997; Barker and Camerlenghi, 2002). Through repeated glaciations the ice sheet has eroded and  
79 over-deepened the inner shelf, extended the outer shelf through progradation and delivered large  
80 volumes of sediment to the deep ocean (Barker and Camerlenghi, 2002; Bart and Iwai, 2012;  
81 Hernández-Molina et al., 2017). The AHT, a 140 km-long by 50 km-wide cross-shelf trough (Fig. 1),  
82 was a recurring ice stream pathway during glacial maxima (Larter and Cunningham, 1993; Larter and  
83 Vanneste, 1995). The most recent grounding zone advance to the shelf edge along the AHT occurred  
84 during the LGM (Pudsey et al., 1994; Heroy and Anderson, 2005; Ó Cofaigh et al., 2014). To the  
85 southeast of the trough, the inner shelf is incised by an erosional basin, Palmer Deep (PD), that  
86 measures 26 km east-to-west and 10 km north-to-south at the 800 m depth contour (Domack et al.,  
87 2006; Fig. 1). PD has a maximum depth >1400 m, yet to both north and south there are small islands  
88 within 12 km of its axis and there is a bank directly to its west that rises to <200 metres below sea  
89 level. Rebesco et al. (1998) and Domack et al. (2006) argued that in colder temperatures than today  
90 and with lower sea level – e.g. at the start of Marine Isotope Stage 2 (29 ka) - ice encroached  
91 towards PD from the nearby land areas and local ice caps formed on emergent platforms around the  
92 present-day islands near the basin. These authors further hypothesized that continued glacial  
93 development led to the PD basin becoming completely encircled by grounded glacial ice and to  
94 formation of an ice shelf over it, trapping a subglacial lake. Based on multibeam bathymetry data  
95 from the inner shelf, Domack et al. (2006) described channels crossing the deepest part of the sill  
96 separating the western end of PD from the AHT that are 200–500 m-wide, 100–300 m deep and  
97 exhibit reversals in their longitudinal profiles. On the basis of these characteristics and similarities to  
98 channels in Pine Island Bay and to the Labyrinth channels in Wright Valley in the Transantarctic  
99 Mountains that had previously been interpreted as having been eroded by subglacial water flow

100 (e.g. Lowe and Anderson, 2003; Nitsche et al., 2013; Lewis et al., 2006), Domack et al. (2006)  
101 interpreted the channels as having been eroded by outflow from a subglacial lake in PD. More  
102 recently, geochemical analysis of pore waters from sediments in one of the basins within the  
103 channel network in Pine Island Bay confirmed that it had been a sub-glacial lake (Kuhn et al., 2017).

104

## 105 **2. Methods**

106

### 107 **2.1 Multibeam bathymetry and acoustic sub-bottom profile data**

108

109 Extensive new data were collected on RRS *James Clark Ross* cruise JR284 in January 2014 using a  
110 1°x1° Kongsberg EM122 system with 432 beams and a transmission frequency in the range 11.25–  
111 12.75 kHz. Beam raypaths and sea bed depths were calculated in near real time using sound velocity  
112 profiles derived from conductivity temperature-depth and expendable bathythermograph casts  
113 made during the cruise. Processing consisted of rejecting outlying values, replacing the sound  
114 velocity profile applied during acquisition with a more relevant one for some data, and gridding to  
115 isometric 30 m cells using a Gaussian weighted mean filter algorithm in MB-System software (Caress  
116 and Chayes, 1996; Caress et al., 2018). Pre-existing multibeam data, mostly collected on RVIB  
117 *Nathaniel B. Palmer* and previous cruises of RRS *James Clark Ross* (Anderson, 2005; Domack, 2005;  
118 Lavoie et al., 2015), and data along a few tracks collected more recently on HMS *Protector* using a  
119 Kongsberg EM710 system (70–100 kHz), were included in the grid. Acoustic sub-bottom echo  
120 sounding profiles were collected along all JR284 survey lines with a Kongsberg TOPAS PS018  
121 parametric system using a 15 ms chirp transmission pulse with secondary frequencies ranging 1.3–5  
122 kHz. Vessel motion and GPS navigation data on cruise JR284 were collected using a Seatex Seapath  
123 200 system.

124

### 125 **2.2 Heritage seismic reflection data**

126

127 MCS data used were collected in the 1980s on RRS *Discovery* cruises D154 and D172 (Larter and  
128 Cunningham, 1993, Larter et al., 1997). On D154, Line AMG845-03 was collected with a 2400 m-long  
129 hydrophone streamer, whereas on D172 the streamer used to collect data on Line BAS878-11 was  
130 800 m in length. In both cases the streamer was towed at 8–10 m depth and data were recorded  
131 from 50 m-long groups with a sampling interval of 4 ms. The seismic source consisted of four airguns  
132 with total volumes of 8.5 l on D154 and 15.8 l on D172, respectively, and data were processed to  
133 common mid-point stack using standard procedures. Very high resolution seismic data were

134 collected using a Hunttec DTB, towed within 100 m of the sea bed, on RRS *James Clark Ross* cruise  
135 JR01 in 1992 (Larter and Vanneste, 1995; Vanneste and Larter, 1995). This system transmitted a  
136 broadband pulse with frequencies 0.8–10 kHz and a cycle time of 0.9 s. Data were recorded with a  
137 100  $\mu$ s sampling interval from a 1 m-long hydrophone trailed behind the towed vehicle. The DTB  
138 system is capable of resolving sedimentary layers <1 m in thickness and also achieves very high  
139 spatial resolution due to the proximity of the source and receiver to the sea bed.

140

### 141 **3. Results**

142

#### 143 **3.1 Description and interpretation of landforms and seismic/acoustic profiles.**

144

145 Integration of the new multibeam bathymetry data with pre-existing data provides nearly  
146 continuous coverage of the AHT from PD to beyond the continental shelf edge, with the new data  
147 spanning the full width of the trough on the middle shelf (Fig. 1). They also include coverage of the  
148 confluence with a tributary trough that joins the AHT from the east on the middle shelf. We will refer  
149 to this tributary by the informal name ‘Perrier Trough’, as it originates offshore from Perrier Bay,  
150 Anvers Island. The data reveal extensive areas of MSGL and drumlins, which are characteristic of ice  
151 stream beds and show the pattern of palaeo-ice flow (Stokes and Clark, 1999; King et al., 2009;  
152 Graham et al., 2009). Fields of drumlins, with elongation ratios between 2.5 and 6:1, occur over a  
153 broad transition zone between the rugged inner shelf and smoother mid-shelf part of the AHT, and  
154 where the AHT crosses a structural high that separates middle and outer shelf areas (Larter et al.,  
155 1997). MSGL in the mid-shelf part of the AHT have elongation ratios between 12 and 17:1, whereas  
156 some on the outer shelf have elongation ratios up to 80:1. The data also confirm the occurrence of  
157 several grounding zone wedges (Fig. 1), some of which had been identified previously, indicating  
158 positions where the grounding zone paused during retreat from its LGM position (Larter and  
159 Vanneste, 1995; Vanneste and Larter, 1995; Batchelor and Dowdeswell, 2015). Here, however, we  
160 focus on two specific areas in which the landforms observed have a bearing on the role of subglacial  
161 hydrology in facilitating and controlling ice stream flow.

162

#### 163 **3.2 Southern Anvers-Hugo Trough**

164

165 In the southern part of the AHT there is a marked along-trough change in landforms across a line  
166 where a MCS profile (AMG845-03) shows that a mid-shelf sedimentary basin pinches out (Figs 2a  
167 and 3), with acoustic basement cropping out to the southeast (Larter et al., 1997). The acoustic

168 basement most likely represents Palaeozoic-Mesozoic igneous and metasedimentary rocks similar to  
169 those that crop out on the nearby islands (Storey and Garrett, 1985; Leat et al., 1995). The  
170 sedimentary strata in the basin are of unknown age, but it has previously been inferred that the  
171 youngest layers could be no younger than middle Miocene and the oldest layers may be early  
172 Tertiary or Late Cretaceous in age (Larter et al., 1997). Crescentic scours around the 'upstream' ends  
173 of bathymetric highs and fields of anastomosing channels are observed in the area where acoustic  
174 basement crops out (Fig. 2a). Among the anastomosing channels, the largest are up to 30 m deep  
175 and 250 m wide, although many are smaller (Fig. 2b).

176 In the axis of the AHT directly north of this zone, incised into the edge of the sedimentary basin,  
177 the new data reveal a set of northward shoaling and narrowing valleys spaced 2–3 km apart (Fig. 2a).  
178 Individual valleys are up to 1100 m wide and 60 m deep at their southern ends (Fig. 2c), but become  
179 narrower and shallower northwards (Fig. 2c,d ), ultimately petering out over a distance of <5 km.  
180 The slope along the steepest part of the channel axes is  $\sim 2^\circ$  (Fig. 2d). In detail, the southern part of  
181 each valley exhibits a v-shaped deeper section incised into a u-shaped upper section, the v-shaped  
182 sections being up to 350 m wide and 45 m deep (Fig. 2c). MSGL start directly north of these valleys  
183 (Figs 2a and 4) and cover most of the sea bed in the trough between this point and the continental  
184 shelf edge.

185 Two acoustic sub-bottom profiles that run transverse to the trough about 8 and 10 km north of  
186 the northern tips of the valleys show that the MSGL were formed in the surface of an acoustically  
187 transparent layer that is draped by a 4 m-thick layer of younger sediments (Fig. 4). Where such  
188 acoustically transparent layers have been cored elsewhere on the West Antarctic shelf they have  
189 been shown to consist of relatively low shear strength, deformed till, dubbed 'soft till', and the high  
190 amplitude reflector below this layer has been shown to correlate with the top of a higher shear  
191 strength 'stiff till' (e.g. Ó Cofaigh et al., 2005a; Reinardy et al., 2011). A homogenous, terrigenous  
192 diamicton with moderate shear strength, which was recovered in marine sediment cores from AHT,  
193 documents the presence of the soft till there (Pudsey et al., 1994; Heroy and Anderson, 2005). Each  
194 of the sub-bottom profiles shows three depressions in this high amplitude reflector that are 8–10 m  
195 deep, 400–800 m wide and contain an acoustically transparent fill, above which a reflector is usually  
196 observed separating the fill from the overlying soft till layer (Fig. 4).

197 We interpret the anastomosing channels and crescentic scours incised into the hard substrate on  
198 the inner shelf as having been eroded by subglacial water flow at times when grounded ice extended  
199 further offshore, as previous authors have interpreted similar features elsewhere (Dreimanis, 1993;  
200 Lowe and Anderson, 2003; Nitsche et al., 2013; Lewis et al., 2006; Graham and Hogan, 2016). This  
201 origin is also consistent with the interpretation that a subglacial lake was present in PD during the

202 last glacial period, and channels incising the sill at its western end were eroded by outflow from the  
203 lake (Domack et al., 2006). Considering the scale of such features here, as well as in other areas  
204 around Antarctica, and the nature of the material they are eroded into, they probably developed  
205 progressively through multiple glacial cycles (Smith et al., 2009; Nitsche et al., 2013). The scale of the  
206 features also implies that water flow rates fast enough to drive erosion can only have been achieved  
207 through subglacial storage of water and episodic discharge (rather than continuous flow), even if it is  
208 assumed that the upper parts of scours and channels were filled with ice (Nitsche et al., 2013;  
209 Kirkham et al., 2019). This is, once again, consistent with the interpretation of a subglacial lake in PD,  
210 and also with a semi-quantitative model that implies outbursts from trapped subglacial lakes in such  
211 settings and of these approximate dimensions are likely to occur with repeat periods of the order of  
212 a few centuries (Alley et al., 2006).

213 A conservative estimate for the volume of the PD subglacial lake stated by Domack et al. (2006)  
214 was 20 km<sup>3</sup>. However, the full volume of the basin deeper than the sill depth of ~500 m is about 110  
215 km<sup>3</sup>. If this was filled the lake would have been nearly two orders of magnitude greater in volume  
216 than subglacial Lake Ellsworth (1.37 km<sup>3</sup>, Woodward et al., 2010), but still nearly two orders of  
217 magnitude smaller than Lake Vostock (5400 ±1600 km<sup>3</sup>, Studinger et al., 2004). The length and width  
218 of PD are similar to Lake Engelhardt, the largest of a number of connected shallow lakes beneath the  
219 lower Mercer and Whillans ice streams, from which remote sensing data show ~2 km<sup>3</sup> of water  
220 drained between October 2003 and June 2006 (Fricker et al., 2007). However, water depth in these  
221 lakes likely rarely exceeds 10 metres (Christianson et al., 2012), so their volumes are small compared  
222 to the potential size of lakes in deep basins such as PD.

223 Considering that the northward-shoaling valleys are located in the axis of the AHT directly north  
224 of an area containing anastomosing channels and crescentic scours, we interpret them as also having  
225 been eroded by subglacial water flow. We interpret the upper u-shaped sections of the valleys (Fig.  
226 2c) as having been widened by glacial erosion, implying that the valleys have been overridden by ice  
227 since they were first carved. This is consistent with the suggestion that many features eroded into  
228 bedrock on Antarctic continental shelves developed through multiple glaciations (Graham et al.,  
229 2009). Even at times when there was active water flow, ice may also have filled a large part of the v-  
230 shaped lower sections. Palaeo-ice flow paths indicated by streamlined bedforms show that the area  
231 in the axis of the AHT where the valleys occur lies directly down flow from the sill at the western end  
232 of PD. MSGL directly north of the valleys indicate that there was fast ice flow in this part of the  
233 trough, likely facilitated by the soft till layer that is seen as an acoustically transparent layer in sub-  
234 bottom profiles (cf. Alley et al., 1986; Ó Cofaigh et al., 2005a; Reinardy et al., 2011). The coincidence  
235 of the onset of MSGL with northward disappearance of the valleys suggests that water supplied

236 through them was important in lubricating and dilating the till, thus reducing its shear strength and  
237 making it more prone to deform under stress. Thus we infer that the northward terminations of the  
238 valleys were associated with a transition from channelized to distributed water flow at the ice bed.  
239 The shallow, filled depressions observed in the sub-bottom profiles (Fig. 4) suggest that the valleys  
240 once continued further to the north, before their distal reaches were filled and the overlying soft till  
241 in which MSGL are formed accumulated beneath fast-flowing ice. The sequence of units observed in  
242 the profiles could have resulted from upstream migration of the onset of sediment-lubricated  
243 streaming flow during the last glaciation.

244

### 245 **3.3 Confluence of Anvers-Hugo and Perrier troughs**

246

247 In the area of the confluence between AHT and Perrier Trough, an area of east-west aligned MSGL  
248 terminates abruptly along a line parallel to their trend on the southern flank of the Perrier Trough  
249 (Fig. 5a). The eastern limit of the area covered by MSGL in AHT is more irregular, but lies within a  
250 band no more than 3 km wide on the eastern flank of the trough. Streamlined bedforms are absent  
251 from the area between the two troughs, but several steep-sided bathymetric basins up to 1500 m  
252 wide and 40 m deep are observed (Fig. 5a-c). The central parts of most basins are flat or gently-  
253 dipping so that cross-sections exhibit box-shaped profiles (Fig. 5b,c). A 500 m-wide and 8 m-high  
254 mound occurs on the north-western side of one of the largest basins (Fig. 5c). A few of the basins  
255 span the boundary of MSGL on the southern flank of Perrier Trough. Furthermore, about 3 km north  
256 of the boundary of MSGL and to the east of the other basins, linear features connect a small basin  
257 ~300 m in diameter with a similarly-sized mound 1.6 km to its WNW (Fig. 5a).

258 We interpret the well-defined southern lateral boundary of MSGL in Perrier Trough as indicating  
259 the marginal shear zone position when the palaeo-ice stream reached its maximum width during the  
260 LGM. Similarly, the lateral limit of MSGL on the eastern flank of the AHT lies within a band that is no  
261 more than 3 km wide, indicating the approximate position of the shear zone at the margin of the  
262 palaeo-ice stream occupying this trough when it was at its widest. Such clear expressions of ice  
263 stream shear margin positions in bed morphology have proved elusive beneath the modern ice  
264 sheet, partly because the chaotic structure of shear zones causes scattering of ice-penetrating radar  
265 signals that is observed as 'clutter' in survey data (Shabtaie and Bentley, 1987). The steep-sided  
266 basins in the area between the two troughs are similar to the holes of hill-hole pairs and scars  
267 resulting from detachment of sediment rafts observed on the northeastern part of the Amundsen  
268 Sea continental shelf (Klages et al., 2013, 2015, 2016). The small mound and basin in the Perrier  
269 Trough 3 km north of the boundary of MSGL appear to be a clear example of a hill-hole pair. Such

270 features are generally regarded as characteristic of erosion and deformation beneath dry-based ice  
271 cover (e.g. Ottesen et al., 2005; Evans et al., 2006). The mound to the northwest of one of the largest  
272 basins may represent a corresponding hill (Fig. 5a, c), although as its cross-sectional area is smaller  
273 than that of the adjacent hole it cannot contain all of the excavated sediment. The absence of  
274 mounds near to some of the other basins may be explained by their close proximity to the palaeo-ice  
275 stream confluence, as the excavated material would only need to have been transported a short  
276 distance into the path of one of the ice streams to be entrained by faster flow. Evidence of hill-hole  
277 pairs having been overridden and eroded by ice after their formation has previously been reported  
278 from the Norwegian continental shelf, where some hills are observed to have streamlined tails (Rise  
279 et al., 2016). The pristine form of the hill-hole pair within the Perrier Trough indicates that it must  
280 have formed after ice stream flow had stagnated.

281 A DTB profile runs across the bathymetric basin that lies closest to the confluence of the two  
282 troughs and, beneath thin, patchily distributed younger sediments, it shows an acoustically  
283 transparent layer up to 25 ms (~20 m) thick (Figs 5a, 6). This layer has a minimum thickness of <3 m  
284 beneath the south-eastern edge of the basin floor, and it thickens progressively to the north-west  
285 across the basin. In places short segments of truncated, dipping reflectors can be seen beneath the  
286 strong reflector at the base of the acoustically transparent layer (Fig. 6). We interpret the  
287 acoustically transparent layer as consisting of Quaternary diamictos overlying an unconformity  
288 above mid-shelf basin sedimentary strata that are represented by the truncated, dipping reflectors.  
289 The reduced thickness of the acoustically transparent layer across the basin suggests that the 'hole'  
290 was formed by erosion of Quaternary diamictos and that the older sedimentary strata were  
291 unaffected during its formation. As mentioned above, such holes are generally regarded as  
292 characteristic of erosion beneath dry-based ice cover, and therefore the restriction of erosion to the  
293 Quaternary diamictos is consistent with the shear stress threshold for brittle failure in them likely  
294 being significantly lower than in the underlying consolidated strata (Evans et al., 2006). At the sea  
295 bed near the foot of the steep south-east flank of the basin, a unit that is 180 m across and 7 ms  
296 (~5.5 m) thick containing south-east dipping reflectors is observed. We interpret this unit as a  
297 rotated slide block that has originated from the flank of the 'hole' after its excavation. The most  
298 prominent reflector within the block is most likely to be from the boundary between diamicton and  
299 postglacial sediment as observed to the NW of the basin (Fig, 6), in which case the displacement of  
300 the block did not occur until after a layer of postglacial sediments several metres in thickness had  
301 accumulated.

302 A MCS profile that runs obliquely across Perrier Trough and continues over the inter-trough area  
303 shows mid-shelf basin sedimentary strata underlying the sea bed along the entire line (Figs 5a, 7). As

304 noted above, the oldest strata in this basin may be as old as Late Cretaceous, but most of the basin  
305 fill is likely of Tertiary age (Larter et al., 1997). The southern lateral limit of MSGL in Perrier Trough  
306 lies within 1 km of the position where a unit of younger strata with a distinct seismic facies character  
307 (labelled 'later mid-shelf basin' in Fig. 7) pinches out, but is not coincident with this boundary.

308

#### 309 **4. Discussion and Conclusions**

310

311 The features described here suggest that subglacial water, likely supplied episodically from a  
312 subglacial lake in PD, played an important role in facilitating ice stream flow in the AHT during the  
313 last and probably several late Quaternary glacial periods, and likely modulated the flow velocity.

314 In the palaeo-ice stream confluence area (Fig. 5a) the close juxtaposition of MSGL, which are  
315 characteristic of wet-based, fast ice flow (Stokes and Clark, 1999; King et al., 2009; Graham et al.,  
316 2009), with excavated basins ('holes') that are characteristic of slow, dry-based ice flow (Ottesen et  
317 al., 2005; Evans et al., 2006), suggests that water availability was an important control on the lateral  
318 extent of the palaeo-ice streams. This interpretation is supported by a MCS profile that shows the  
319 palaeo-ice stream shear margin position on the south side of Perrier Trough does not coincide with a  
320 major geological boundary (Fig. 7). The MCS profile shows that the Perrier Trough palaeo-ice stream  
321 and the inter-stream area are both underlain by dipping sedimentary strata of likely Tertiary age.  
322 The position of the shear margin does, however, lie within 1 km of a second-order boundary  
323 between strata of different ages and with different seismic facies that may have had some influence  
324 on its position (Fig. 7). Unfortunately, available seismic profiles are too widely spaced to assess how  
325 closely the palaeo-shear margin follows this boundary.

326 The observation that a few of the 'holes', and one clear hill-hole pair, span the boundary of, and  
327 cross-cut, MSGL on the southern flank of Perrier Trough suggests inward ice stream shear margin  
328 migration during glacial recession. Lateral migration of shear margins was inferred in the area near  
329 the grounding on the modern Thwaites Glacier between 1996–2000 (Rignot et al., 2002), although a  
330 later study concluded that there had been no significant migration of the eastern shear margin of  
331 the glacier during the most recent two decades (MacGregor et al., 2013). On different parts of the  
332 northern shear margin of Whillans Ice Stream, migration rates of up to  $280 \text{ ma}^{-1}$  outwards and up to  
333  $170 \text{ ma}^{-1}$  inwards were measured over the decade to 1997 (Stearns et al., 2005). Ice-penetrating  
334 radar data across the northern margin of Kamb Ice Stream suggest abrupt inward migration of the  
335 margin  $\sim 200$  years before complete stagnation flow, attributed to reduced lubrication (Catania et al.,  
336 2006). Reduction in basal water supply could occur due to depletion of upstream reservoirs (cf.  
337 Christoffersen et al., 2014), due to surface slope reduction leading to subglacial flow

338 change/reversal, or due to ice thinning or decreasing flow rate and consequent reduction in  
339 pressure melting or strain heating, respectively. Alternatively, in the case of palaeo-ice streams on  
340 continental shelves, reduction in basal water supply could have resulted from total evacuation of  
341 subglacial lakes trapped during ice advance at the LGM. The recovery of tills older than 13 cal. ka BP  
342 at the bases of sediment cores from PD indicates that the lake there was eventually evacuated  
343 (Barker & Camerlenghi 2002; Domack et al. 2001, 2006). However, water discharged from PD would  
344 not have supplied the bed of the palaeo-ice stream in Perrier Trough, so lake evacuation could only  
345 explain decreased water supply there if subglacial lakes were trapped in other deep basins upstream  
346 of the area studied.

347 The onset of MSGL in AHT coincides with the downstream termination of the northward shoaling  
348 valleys. This spatial coincidence suggests that water delivered through the channels played a role in  
349 promoting streaming ice flow northward of this point. The upstream dip of  $2^\circ$  along the steepest  
350 part of the channels (Fig. 2d) implies the minimum ice surface gradient required to produce a basal  
351 hydrological pressure gradient that would drive water northward along the valleys was only  $0.2^\circ$ ,  
352 which is within the range of surface gradients on many modern ice streams (Horgan and  
353 Anandakrishnan, 2006). Water that flowed along the valleys may have been either incorporated into  
354 the till layer that the MSGL formed in, thereby dilating it and facilitating shear deformation, or  
355 dissipated into a thin film that spread along the ice-sediment interface (cf. Ó Cofaigh et al., 2005a).  
356 The sudden appearance of MSGL at this point also requires a source for the till itself, and the most  
357 obvious candidate is the underlying strata at the edge of the sedimentary basin (Fig. 3). Although  
358 these strata have never been sampled they are the most likely source of reworked Cretaceous  
359 radiolarians found in diamictons recovered by drilling on the outer shelf (Shipboard Scientific Party,  
360 1999). Onset of MSGL where ice flowed onto a bed consisting of older sedimentary strata has also  
361 been reported in other locations (e.g. Wellner et al., 2001, 2006, Graham et al., 2009). Erosion of  
362 material from underlying sedimentary strata by, or in the presence of, subglacial water flow presents  
363 a potential mechanism for generating a dilated basal till layer of the kind that has been shown to be  
364 present beneath some modern ice streams (e.g. Alley et al., 1986; Smith, 1997).

365 Subglacial lakes in deep inshore basins such as PD are likely to form during an ice sheet growth  
366 phase (Domack et al., 2006; Alley et al., 2006). In this case, episodes of water expulsion from PD may  
367 have accelerated ice flow and thus contributed to rapid advance of grounded ice with a low surface  
368 gradient across the shelf. Acceleration of ice flow by about 10% over 14 months was observed on  
369 Byrd Glacier following a drainage event from subglacial lakes 200 km upstream of the grounding line  
370 (Stearns et al., 2008), and subglacial meltwater drainage flux and routing is also known to influence  
371 flow rates of glaciers in Greenland (Sundal et al., 2011). The axis of AHT shallows steadily from >600

372 m where MSGL start on the middle shelf to <440 m at the shelf edge (Vanneste and Larter, 1995),  
373 and grounding lines are potentially unstable on such upstream-deepening beds (Weertman, 1974;  
374 Schoof, 2007; Katz and Worster, 2010). Therefore, if episodic subglacial water outbursts caused  
375 'surging' ice stream behaviour, as envisaged by Alley et al. (2006), they may also have resulted in  
376 fluctuations in grounding line positions.

377 Our interpretations are consistent with the hypothesis that subglacial lakes or areas of elevated  
378 geothermal heat flux play a critical role in the onset of many large ice streams (Bell, 2008). There are  
379 other deep, steep-sided inner shelf basins where subglacial lakes could have been trapped during  
380 glacial advance in the catchment areas of several other well-documented Antarctic palaeo-ice  
381 streams. For example, there are several basins >900 m deep in Marguerite Bay, which is part of the  
382 catchment of the Marguerite Trough palaeo-ice stream (Livingstone et al., 2013; Arndt et al., 2013),  
383 and there is a >1100 m-deep basin in Eltanin Bay at the head of the Belgica Trough palaeo-ice stream  
384 (Ó Cofaigh et al., 2005b; Graham et al., 2011; Arndt et al., 2013). In the Amundsen Sea Embayment,  
385 there are >1500 m-deep inner shelf basins in the catchments of both the Pine Island-Thwaites and  
386 Dotson-Getz palaeo-ice streams (Larter et al., 2009; Graham et al., 2009, 2016; Nitsche et al., 2013;  
387 Arndt et al., 2013; Witus et al., 2014), and it has been shown that at least one of those in the former  
388 area did indeed host a sub-glacial lake (Kuhn et al., 2017). Hence subglacial lakes at the onset of  
389 many continental shelf palaeo-ice streams may have facilitated their advance across the shelf during  
390 late Quaternary glacial periods. Furthermore, if the lakes persisted when the ice streams had  
391 advanced to the outer shelf, outbursts from them could have caused surge-like behaviour leading to  
392 fluctuations in grounding line positions on typical inward-deepening Antarctic continental shelf  
393 areas. Such behaviour of marine-based palaeo-ice streams on timescales of the order of centuries, as  
394 suggested by the simple model proposed by Alley et al. (2006), could explain the observation of  
395 cross-cutting MSGL in several outer continental shelf areas (e.g. Ó Cofaigh et al., 2005a, 2005b;  
396 Mosola and Anderson, 2006). The preservation of MSGL from successive flow phases precludes  
397 erosion or deposition of more than a few metres of sediment between them, which is easier to  
398 envisage if the time separation between the flow phases is relatively small. The potential for such  
399 subglacial lake outbursts to recur at decadal to centennial intervals and to cause significant ice  
400 dynamic fluctuations means that there is a need to better understand the processes involved in  
401 order to better forecast the future behaviour of modern ice streams and the contribution they will  
402 make to sea-level change.

403

404 *Data availability.* The multibeam bathymetry grid is available online from the NERC Polar Data  
405 Centre (doi:[DOI NUMBER TO BE ADVISED]). The raw multibeam data and acoustic sub-bottom

406 profiler data collected on cruise JR284, as well as the heritage seismic data, are available on request  
407 from the NERC Polar Data Centre. Stacked MCS data from line AMG845-03 are available from the  
408 Scientific Committee on Antarctic Research Seismic Data Library System.

409

410 *Author contributions.* RDL conceived the idea for the study and together with C-DH, JAS, JAD, KAH  
411 and AGCG developed the research plan for cruise JR284. RDL together with KAH, C-DH and JAS wrote  
412 the manuscript. RDL, KAH, AJT, CLB, C-DH, JAS and MC collected the multibeam bathymetry and  
413 acoustic sub-bottom profile data on cruise JR284. JDK, ZAR, GK, AGCG and JAD participated in  
414 discussions with the aforementioned authors on interpretation of the data and their implications for  
415 subglacial hydrological systems. All authors commented on the manuscript and provided input to its  
416 final version.

417

418 *Competing interests.* The authors declare that they have no conflict of interest.

419

420 *Acknowledgements.* We thank the captain, officers and crew on RRS *James Clark Ross* cruise JR284,  
421 and Elanor Gowland and Ove Meisel who assisted with data collection. We also thank the captain,  
422 hydrographers, officers and crew who sailed on HMS *Protector* during the 2015-16 and 2016-17  
423 Antarctic seasons, from which additional data were incorporated. Heritage data collected on RVIB  
424 *Nathaniel B. Palmer* were obtained from the Marine Geoscience Data System ([www.marine-geo.org](http://www.marine-geo.org)). The MCS data on line BAS878-11 were processed by Alex Cunningham, and Christian dos  
425 Santos Ferreira provided valuable help and advice in using MB-System to suppress some artefacts.  
426 This study is part of the Polar Science for Planet Earth Programme of the British Antarctic Survey.  
427 Participation of KAH, CLB and MC on cruise JR284 was funded by Natural Environment Research  
428 Council Collaborative Gearing Scheme awards. We thank Huw Horgan and an anonymous reviewer  
429 for helpful reviews that improved the paper.

431

432

433 **References**

- 434 Alley, R. B., Blankenship, D. D., Bentley, C. R., and Rooney, S. T.: Deformation of till beneath ice  
435 stream B, West Antarctica, *Nature*, 322, 57–59, 1986.
- 436 Alley, R. B., Dupont, T. K., Parizek, B. R., Anandakrishnan, S., Lawson, D. E., Larson, G. J., and Evenson,  
437 E. B.: Outburst flooding and the initiation of ice-stream surges in response to climatic cooling: A  
438 hypothesis, *Geomorphology*, 75, 76–89, 2006.
- 439 Anderson, J.: Processed Multibeam Sonar Data (version 2) near the Antarctic Peninsula acquired  
440 during Nathaniel B. Palmer expedition NBP0201 (2002), Interdisciplinary Earth Data Alliance  
441 (IEDA), <https://doi.org/10.1594/IEDA/100309>, 2005.
- 442 Arndt, J. E., Schenke, H. W., Jakobsson, M., Nitsche, F. O., Buys, G., Goleby, B., Rebesco, M., Bohoyo,  
443 F., Hong, J., Black, J., Greku, R., Udintsev, G., Barrios, F., Reynoso-Peralta, W., Taisei, M., and  
444 Wigley, R.: The International Bathymetric Chart of the Southern Ocean (IBCSO) Version 1.0—A  
445 new bathymetric compilation covering circum-Antarctic waters, *Geophys. Res. Lett.*, 40, 3111–  
446 3117, <https://doi.org/10.1002/grl.504132013>, 2013.
- 447 Barker, P. F. and Camerlenghi, A.: Glacial history of the Antarctic Peninsula from Pacific margin  
448 sediments, in: *Antarctic Glacial History and Sea-Level Change*, edited by: Barker, P. F.,  
449 Camerlenghi, A., Acton, G. D., and Ramsay, A. T. S., *Proceedings of the Ocean Drilling Program,*  
450 *Scientific Results*, [Online], 2002), vol. 178, 1–40, [https://www-](https://www-odp.tamu.edu/publications/178_SR/synth/synth.htm)  
451 [odp.tamu.edu/publications/178\\_SR/synth/synth.htm](https://www-odp.tamu.edu/publications/178_SR/synth/synth.htm), 2002.
- 452 Bart, P. J. and Iwai, M.: The overdeepening hypothesis: How erosional modification of the marine-  
453 scape during the early Pliocene altered glacial dynamics on the Antarctic Peninsula's Pacific  
454 margin, *Palaeogeogr. Palaeoclimatol. Palaeoecol.* 335–336, 42–51,  
455 <https://doi.org/10.1016/j.palaeo.2011.06.010>, 2012.
- 456 Batchelor, C. L. and Dowdeswell, J. A.: Ice-sheet grounding-zone wedges (GZWs) on high-latitude  
457 continental margins, *Mar. Geol.*, 363, 65–92, <https://dx.doi.org/10.1016/j.margeo.2015.02.001>,  
458 2015.
- 459 Bell, R. E.: The role of subglacial water in ice-sheet mass balance, *Nat. Geosci.*, 1, 297–304,  
460 <https://doi.org/10.1038/ngeo186>, 2008.
- 461 Bell, R. E., Studinger, M., Shuman, C. A., Fahnestock, M. A., and Joughin, I.: Large subglacial lakes in  
462 East Antarctica at the onset of fast-flowing ice streams. *Nature*, 445, 904–907,  
463 <https://doi.org/10.1038/nature05554>, 2007.
- 464 Caress, D. W. and Chayes, D. N.: Improved processing of Hydrosweep DS multibeam data on the R/V  
465 Maurice Ewing, *Mar. Geophys. Res.*, 18, 631–650, 1996.

466 Caress, D. W., Chayes, D. N., and dos Santos Ferreira, C.: MB-System: Mapping the Seafloor,  
467 <https://www.mbari.org/products/research-software/mb-system>, 2018.

468 Catania, G. A., Scambos, T. A., Conway, H., and Raymond, C. H.: Sequential stagnation of Kamb Ice  
469 Stream, West Antarctica, *Geophys. Res. Lett.*, 33, L14502,  
470 <https://doi.org/10.1029/2006GL026430>, 2006.

471 Christianson, K., Jacobel, R. W., Horgan, H. J., Anandakrishnan, S., and Alley, R. B.: Subglacial Lake  
472 Whillans – Ice-penetrating radar and GPS observations of a shallow active reservoir beneath a  
473 West Antarctic ice stream, *Earth Planet. Sci. Lett.*, 331–332, 237–245,  
474 <https://doi.org/10.1016/j.epsl.2012.03.013>, 2012.

475 Christianson, K., Peters, L. E., Alley, R. B., Anandakrishnan, S., Jacobel, R. W., Riverman, K. L., Muto,  
476 A., and Keisling, B. A.: Dilatant till facilitates ice-stream flow in northeast Greenland, *Earth  
477 Planet. Sci. Lett.*, 401, 57–69, <https://doi.org/10.1016/j.epsl.2014.05.060>, 2014.

478 Christoffersen, P., Bougamont, M., Carter, S. P., Fricker, H. A., and Tulaczyk, S.: Significant  
479 groundwater contribution to Antarctic ice streams hydrologic budget, *Geophys. Res. Lett.*, 41,  
480 2003–2010, <https://doi.org/10.1002/2014GL059250>, 2014.

481 Domack, E.: Processed Multibeam Sonar Data (version 2) near the Antarctic Peninsula acquired  
482 during Nathaniel B. Palmer expedition NBP0107 (2001), Interdisciplinary Earth Data Alliance  
483 (IEDA), <https://doi.org/10.1594/IEDA/100307>, 2005.

484 Domack, E., Leventer, A., Dunbar, R., Taylor, F., Brachfeld, S., and Sjunneskog, C.: Chronology of the  
485 Palmer Deep site, Antarctic Peninsula: a Holocene palaeoenvironmental reference for the  
486 circum-Antarctic. *The Holocene*, 11, 1–9, <https://doi.org/10.1191/095968301673881493>, 2001.

487 Domack, E. W., Amblàs, D., Gilbert, R., Brachfeld, S., Camerlenghi, A., Rebesco, M., Canals, M., and  
488 Urgeles, R.: Subglacial morphology and glacial evolution of the Palmer deep outlet system,  
489 Antarctic Peninsula, *Geomorphology*, 75, 125–142,  
490 <https://doi.org/10.1016/j.geomorph.2004.06.013>, 2006.

491 Dreimanis, A.: Water-eroded crescentic scours and furrows associated with subglacial flutes at  
492 Breidamerkurjökull, Iceland, *Boreas*, 22, 110–112, [https://doi.org/10.1111/j.1502-  
493 3885.1993.tb00170.x](https://doi.org/10.1111/j.1502-3885.1993.tb00170.x), 1993.

494 Dowdeswell, J. A., Canals, M., Jakobsson, M., Todd, B. J., Dowdeswell, E. K., and Hogan, K. A.:  
495 Introduction: an atlas of submarine glacial landforms, in: *Atlas of Submarine Glacial Landforms:  
496 Modern, Quaternary and Ancient*, edited by Dowdeswell, J. A., Canals, M., Jakobsson, M., Todd,  
497 B. J., Dowdeswell, E. K., and Hogan, K. A., *Memoirs, Geological Society, London*, vol. 46, 3–14,  
498 <https://doi.org/10.1144/M46.171>, 2016.

499 Evans, D. J. A., Phillips, E. R., Hiemstra, J. F., and Auton, C. A.: Subglacial till: formation, sedimentary  
500 characteristics and classification, *Earth-Sci. Rev.*, 78, 115–176,  
501 <https://doi.org/10.1016/j.earscirev.2006.04.001>, 2006.

502 Fahnestock, M., Abdalati, W., Joughin, I., Brozena, J., and Gogineni, P.: High geothermal heat flow,  
503 basal melt, and the origin of rapid ice flow in central Greenland, *Science*, 294, 2338–2342, 2001.

504 Fricker, H. A., Scambos, T., Bindschadler, R., and Padman, L.: An active subglacial water system in  
505 West Antarctica mapped from space, *Science*, 315, 1544–1548, 2007.

506 Graham, A. G. C. and Hogan, K. A.: Crescentic scours on palaeo-ice stream beds, in: *Atlas of*  
507 *Submarine Glacial Landforms: Modern, Quaternary and Ancient*, edited by Dowdeswell, J. A.,  
508 Canals, M., Jakobsson, M., Todd, B. J., Dowdeswell, E. K., and Hogan, K. A., *Memoirs, Geological*  
509 *Society, London*, vol. 46, 221–222, <https://doi.org/10.1144/M46.166>, 2016.

510 Graham, A. G. C., Larter, R. D., Gohl, K., Hillenbrand, C.-D., Smith, J. A., and Kuhn, G.: Bedform  
511 signature of a West Antarctic palaeo-ice stream reveals a multi-temporal record of flow and  
512 substrate control, *Quat. Sci. Rev.*, 28, 2774–2793,  
513 <https://doi.org/10.1016/j.quascirev.2009.07.003>, 2009.

514 Graham, A. G. C., Nitsche, F. O., and Larter, R. D.: An improved bathymetry compilation for the  
515 Bellingshausen Sea, Antarctica, to inform ice-sheet and ocean models, *The Cryosphere*, 5, 95–  
516 106, <https://doi.org/10.5194/tc-5-95-2011>, 2011.

517 Graham, A. G. C., Jakobsson, M., Nitsche, F. O., Larter, R. D., Anderson, J. B., Hillenbrand, C.-D., Gohl,  
518 K., Klages, J. P., Smith, J. A., and Jenkins, A.: Submarine glacial-landform distribution across the  
519 West Antarctic margin, from grounding line to slope: the Pine Island–Thwaites ice-stream  
520 system, in: *Atlas of Submarine Glacial Landforms: Modern, Quaternary and Ancient* edited by  
521 Dowdeswell, J. A., Canals, M., Jakobsson, M., Todd, B. J., Dowdeswell, E. K., and Hogan, K. A.,  
522 *Memoirs, Geological Society, London*, vol. 46, 493–500, <https://doi.org/10.1144/M46.173>, 2016.

523 Hernández-Molina, F. J., Larter, R. D., and Maldonado, A.: Neogene to Quaternary Stratigraphic  
524 Evolution of the Antarctic Peninsula, Pacific Margin offshore of Adelaide Island: transitions from  
525 a non-glacial, through glacially-influenced to a fully glacial state, *Global Planet. Change*, 156, 80–  
526 111, <https://doi.org/10.1016/j.gloplacha.2017.07.002>, 2017.

527 Heroy, D. C. and Anderson, J. B.: Ice-sheet extent of the Antarctic Peninsula region during the Last  
528 Glacial Maximum (LGM)—Insights from glacial geomorphology, *Geol. Soc. Am. Bull.*, 117, 1497–  
529 1512, 2005.

530 Horgan, H. J. and Anandkrishnan, S.: Static grounding lines and dynamic ice streams: Evidence from  
531 the Siple Coast, West Antarctica, *Geophys. Res. Lett.* 33, L18502,  
532 <https://doi.org/10.1029/2006GL027091>, 2006.

533 Katz, R. F. and Worster, M. G.: Stability of ice-sheet grounding lines, *Proc. Royal Soc. A*, 466, 1597–  
534 1620, <https://doi.org/10.1098/rspa.2009.0434>, 2010.

535 King, E. C., Hindmarsh, R. C. A., and Stokes, C. R.: Formation of mega-scale glacial lineations observed  
536 beneath a West Antarctic ice stream, *Nat. Geosci.*, 2, 585–588,  
537 <https://doi.org/10.1038/NGEO581>, 2009.

538 Kirkham, J. D., Hogan, K. A., Larter, R. D., Arnold, N., Nitsche, F. O., Gollledge, N., and Dowdeswell, J.  
539 A.: Past water flow beneath Pine Island and Thwaites Glaciers, West Antarctica, *The Cryosphere*  
540 *Discussions*, <https://doi.org/10.5194/tc-2019-67>, 2019.

541 Klages, J. P., Kuhn, G., Hillenbrand, C.-D., Graham, A. G. C., Smith, J. A., Larter, R. D., and Gohl, K.:  
542 First geomorphological record and glacial history of an inter-ice stream ridge on the West  
543 Antarctic continental shelf, *Quat. Sci. Rev.*, 61, 47–61,  
544 <https://doi.org/10.1016/j.quascirev.2012.11.007>, 2013.

545 Klages, J. P., Kuhn, G., Graham, A. G. C., Hillenbrand, C.-D., Smith, J. A., Nitsche, F. O., Larter, R. D.,  
546 and Gohl, K.: Palaeo-ice stream pathways and retreat style in the easternmost Amundsen Sea  
547 Embayment, West Antarctica, revealed by combined multibeam bathymetric and seismic data,  
548 *Geomorphology*, 245, 207–222, <https://doi.org/10.1016/j.geomorph.2015.05.020>, 2015.

549 Klages, J. P., Kuhn, G., Hillenbrand, C.-D., Graham, A. G. C., Smith, J. A., Larter, R. D., and Gohl, K.: A  
550 glacial landform assemblage from an inter-ice stream setting in the eastern Amundsen Sea  
551 Embayment, West Antarctica, in: *Atlas of Submarine Glacial Landforms: Modern, Quaternary*  
552 *and Ancient* edited by Dowdeswell, J. A., Canals, M., Jakobsson, M., Todd, B. J., Dowdeswell, E.  
553 K., and Hogan, K. A., *Memoirs, Geological Society, London*, vol. 46, 349–352,  
554 <https://doi.org/10.1144/M46.147>, 2016.

555 Kuhn, G., Hillenbrand, C.-D., Kasten, S., Smith, J. A., Nitsche, F. O., Frederichs, T., Wiers, S., Ehrmann,  
556 W., Klages, J. P., and Mogollón, J. M.: Evidence for a palaeo-subglacial lake on the Antarctic  
557 continental shelf, *Nat. Commun.*, 8, 15591, <https://doi.org/10.1038/ncomms15591>, 2017.

558 Larter, R. D. and Cunningham, A. P.: The depositional pattern and distribution of glacial–interglacial  
559 sequences on the Antarctic Peninsula Pacific margin, *Mar. Geol.*, 109, 203–219, 1993.

560 Larter, R. D. and Vanneste, L. E.: Relict subglacial deltas on the Antarctic Peninsula outer shelf,  
561 *Geology*, 23, 33–36, 1995.

562 Larter, R. D., Rebesco, M., Vanneste, L. E., Gambôa, L. A. P., and Barker, P. F.: Cenozoic tectonic,  
563 sedimentary and glacial history of the continental shelf west of Graham Land, Antarctic  
564 Peninsula, in: *Geology and Seismic Stratigraphy of the Antarctic Margin*, 2, edited by Barker, P. F.  
565 and Cooper, A. K., *Antarctic Research Series, American Geophysical Union, Washington, DC*, vol.  
566 71, 1–27, 1997.

567 Larter, R. D., Graham, A. G. C., Gohl, K., Kuhn, G., Hillenbrand, C.-D., Smith, J. A., Deen, T. J.,  
568 Livermore, R. A., and Schenke, H.-W.: Subglacial bedforms reveal complex basal regime in a zone  
569 of paleo-ice stream convergence, Amundsen Sea Embayment, West Antarctica, *Geology*, 37,  
570 411–414, <https://doi.org/10.1130/G25505A.1>, 2009.

571 Lavoie, C., Domack, E. W., Pettit, E. C., Scambos, T. A., Larter, R. D., Schenke, H.-W., Yoo, K. C., Gutt,  
572 J., Wellner, J., Canals, M., Anderson, J. B., and Amblas, D.: Configuration of the Northern  
573 Antarctic Peninsula Ice Sheet at LGM based on a new synthesis of seabed imagery, *The*  
574 *Cryosphere*, 9, 613–629, <https://doi.org/10.5194/tc-9-613-2015>, 2015.

575 Leat, P. T., Scarrow, J. H., and Millar, I. L.: On the Antarctic Peninsula batholiths, *Geol. Mag.*, 132,  
576 399–412, 1995.

577 Lewis, A. R., Marchant, D. R., Kowalewski, D. E., Baldwin, S. L., and Webb, L. E.: The age and origin of  
578 the Labyrinth, western Dry Valleys, Antarctica: Evidence for extensive middle Miocene subglacial  
579 floods and freshwater discharge to the Southern Ocean, *Geology*, 34, 513–516,  
580 <https://doi.org/10.1130/G22145.1>, 2006.

581 Livingstone, S. J., Ó Cofaigh C., Stokes, C. R., Hillenbrand, C.-D., Vieli, A., and Jamieson, S. S. R.:  
582 Glacial geomorphology of Marguerite Bay Palaeo-Ice stream, western Antarctic Peninsula, *J.*  
583 *Maps*, 9, 558–572, <https://doi.org/10.1080/17445647.2013.829411>, 2013.

584 Lowe, A. L. and Anderson, J. B.: Evidence for abundant subglacial meltwater beneath the paleo-ice  
585 sheet in Pine Island Bay, Antarctica, *J. Glaciol.*, 49, 125–138, 2003.

586 MacGregor, J. A., Catania, G. A., Conway, H., Schroeder, D. M., Joughin, I., Young, D. A., Kempf, S. D.,  
587 and Blankenship, D. D.: Weak bed control of the eastern shear margin of Thwaites Glacier, West  
588 Antarctica, *J. Glaciol.*, 59, 900–912, <https://doi.org/10.3189/2013JoG13J050>, 2013.

589 Mosola, A. B., and Anderson, J. B.: Expansion and rapid retreat of the West Antarctic Ice Sheet in  
590 eastern Ross Sea: possible consequence of over-extended ice streams?, *Quat. Sci. Rev.*, 25,  
591 2177–2196, <https://doi.org/10.1016/j.quascirev.2005.12.013>, 2006.

592 Nitsche, F. O., Gohl, K., Larter, R. D., Hillenbrand, C.-D., Kuhn, G., Smith, J. A., Jacobs, S., Anderson, J.  
593 B., and Jakobsson, M.: Paleo ice flow and subglacial meltwater dynamics in Pine Island Bay, West  
594 Antarctica, *Cryosphere*, 7, 249–262, <https://doi.org/10.5194/tc-7-249-2013>, 2013.

595 Ó Cofaigh C., Pudsey, C. J., Dowdeswell, J. A., and Morris, P.: Evolution of subglacial bedforms along  
596 a paleo-ice stream, Antarctic Peninsula continental shelf, *Geophys. Res. Lett.*, 29, 1199,  
597 <https://doi.org/10.1029/2001GL014488>, 2002.

598 Ó Cofaigh, C., Dowdeswell, J. A., Allen, C. S., Hiemstra, J., Pudsey, C. J., Evans, J., and Evans, D. J. A.:  
599 Flow dynamics and till genesis associated with a marine-based Antarctic palaeo-ice stream,  
600 *Quat. Sci. Rev.*, 24, 709–740, <https://doi.org/10.1016/j.quascirev.2004.10.006>, 2005a.

601 Ó Cofaigh C., Larter, R. D., Dowdeswell, J. A., Hillenbrand, C.-D., Pudsey, C. J., Evans, J., and Morris,  
602 P.: Flow of the West Antarctic Ice Sheet on the continental margin of the Bellingshausen Sea at  
603 the Last Glacial Maximum, *J. Geophys. Res.*, 110, B11103,  
604 <https://doi.org/10.1029/2005JB003619>, 2005b.

605 Ó Cofaigh C., Dowdeswell, J. A., Evans, J., and Larter, R. D.: Geological constraints on Antarctic  
606 palaeo-ice-stream retreat, *Earth Surf. Proc. and Landforms*, 33, 513–525,  
607 <https://doi.org/10.1002/esp.1669>, 2008.

608 Ó Cofaigh C., Davies, B. J., Livingstone, S. J., Smith, J. A., Johnson, J. S., Hocking, E. P., Hodgson, D. A.,  
609 Anderson, J. B., Bentley, M. J., Canals, M., Domack, E., Dowdeswell, J. A., Evans, J., Glasser, N. F.,  
610 Hillenbrand, C.-D., Larter, R. D., Roberts, S. J., and Simms, A. R.: Reconstruction of ice-sheet  
611 changes in the Antarctic Peninsula since the Last Glacial Maximum, *Quat. Sci. Rev.*, 100, 87–110,  
612 <https://doi.org/10.1016/j.quascirev.2014.06.023>, 2014.

613 Ottesen, D., Dowdeswell, J. A., and Rise, L.: Submarine landforms and the reconstruction of fast-  
614 flowing ice streams within a large Quaternary ice sheet: the 2500-km long Norwegian Svalbard  
615 margin (57° to 80° N), *Geol. Soc. Am. Bull.*, 117, 1033–1050, <https://doi.org/10.1130/B25577.1>,  
616 2005.

617 Pudsey, C. J., Barker, P. F., and Larter, R. D.: Ice sheet retreat from the Antarctic Peninsula shelf,  
618 *Continental Shelf Res.*, 14, 1647–1675, 1994.

619 Rebesco, M., Camerlenghi, A., DeSantis, L., Domack, E. W., and Kirby, M.: Seismic stratigraphy of  
620 Palmer Deep: a fault-bounded late Quaternary sediment trap on the inner continental shelf,  
621 Antarctic Peninsula margin, *Mar. Geol.*, 151, 89–110, 1998.

622 Reinardy, B. I., Larter, R. D., Hillenbrand, C.-D., Murray, T., Hiemstra, J. F., and Booth, A. D.:  
623 Streaming flow of an Antarctic Peninsula palaeo-ice stream, both by basal sliding and  
624 deformation of substrate, *J. Glaciol.*, 57, 596–608,  
625 <https://doi.org/10.3189/002214311797409758>, 2011.

626 Rignot, E., Vaughan, D. G., Schmeltz, M., Dupont, T., and MacAyeal, D.: Acceleration of Pine Island  
627 and Thwaites Glaciers, West Antarctica, *Ann. Glaciol.*, 34, 189–194, 2002.

628 Rise, L., Bellec, L. V., Ottesen, D., Bøe, R., and Thorsnes, T.: Hill-hole pairs on the Norwegian  
629 continental shelf, in: *Atlas of Submarine Glacial Landforms: Modern, Quaternary and Ancient*,  
630 edited by Dowdeswell, J. A., Canals, M., Jakobsson, M., Todd, B. J., Dowdeswell, E. K., and Hogan,  
631 K. A., *Memoirs, Geological Society, London*, vol. 46, 203–204, <https://doi.org/10.1144/M46.42>,  
632 2016.

633 Schoof, C.: Ice sheet grounding line dynamics: Steady states, stability, and hysteresis, *J. Geophys.*  
634 *Res.*, 112, F03S28, <https://doi.org/10.1029/2006JF000664>, 2007.

635 Siegfried, M. R., Fricker, H. A., Carter, S. P., and Tulczyk, S.: Episodic ice velocity fluctuations triggered  
636 by a subglacial flood in West Antarctica, *Geophys. Res. Lett.*, 43, 2640–2648,  
637 <https://doi.org/10.1002/2016GL067758>, 2016.

638 Shabtaie, S., and Bentley, C. R.: West Antarctic ice streams draining into the Ross Ice Shelf:  
639 configuration and mass balance. *J. Geophys. Res.*, 92, 1311–1336, 1987.

640 Shipboard Scientific Party: Shelf Transect (Sites 1100, 1102, and 1103), in: *Proc. ODP, Init. Repts.*,  
641 178, edited by Barker, P. F., Camerlenghi, A., Acton, G. D., et al., 1–83 [Online]. Available from  
642 World Wide Web:  
643 <[http://www-odp.tamu.edu/publications/178\\_IR/VOLUME/CHAPTERS/CHAP\\_09.PDF](http://www-odp.tamu.edu/publications/178_IR/VOLUME/CHAPTERS/CHAP_09.PDF)>.  
644 [Cited 2019-04-23], 1999.

645 Smith, A. M.: Basal conditions on Rutford Ice Stream, West Antarctica, from seismic observations, *J.*  
646 *Geophys. Res.*, 102, 543–552, 1997.

647 Smith, J. A., Hillenbrand, C.-D., Larter, R. D., Graham, A. G. C., and Kuhn, G.: The sediment infill of  
648 subglacial meltwater channels on the West Antarctic continental shelf. *Quat. Res.*, 71, 190–200,  
649 <https://doi.org/10.1016/j.yqres.2008.11.005>, 2009.

650 Stearns, L. A., Jezek, K. C., and Van der Veen, C. J.: Decadal-scale variations in ice flow along Whillans  
651 Ice Stream and its tributaries, West Antarctica, *J. Glaciol.*, 51, 147–157, 2005.

652 Stearns, L. A., Smith, B. E., and Hamilton, G. S.: Increased flow speed on a large East Antarctic outlet  
653 glacier caused by subglacial floods, *Nat. Geosci.*, 1, 827–831, <https://doi.org/10.1038/ngeo356>,  
654 2008.

655 Stokes, C. R. and Clark, C. D.: Geomorphological criteria for identifying Pleistocene ice streams, *Ann.*  
656 *Glaciol.*, 28, 67–75, 1999.

657 Storey, B. C. and Garrett, S. W.: Crustal growth of the Antarctic Peninsula by accretion, magmatism  
658 and extension, *Geol. Mag.*, 122, 5–14, 1985.

659 Studinger, M., Bell, R. E., and Tikku, A. A.: Estimating the depth and shape of subglacial Lake Vostok's  
660 water cavity from aerogravity data, *Geophys. Res. Lett.*, 31, L12401,  
661 <https://doi.org/10.1029/2004GL019801>, 2004.

662 Sundal, A. V., Shepherd, A., Nienow, P., Hanna, E., Palmer, S., and Huybrechts, P.: Melt-induced  
663 speed-up of Greenland ice sheet offset by efficient subglacial drainage, *Nature*, 469, 521–524,  
664 <https://doi.org/10.1038/nature09740>, 2011.

665 Vanneste, L. E and Larter, R. D.: Deep-tow boomer survey on the Antarctic Peninsula Pacific margin:  
666 An investigation of the morphology and acoustic characteristics of late Quaternary sedimentary  
667 deposits on the outer continental shelf and upper slope, in: *Geology and Seismic Stratigraphy of*

668 the Antarctic Margin, edited by Cooper, A. K., Barker, P. F., and Brancolini, G., Antarctic Research  
669 Series, American Geophysical Union, Washington, DC, vol. 68, 97–121, 1995.

670 Wellner, J. S., Lowe, A. L., Shipp, S. S., and Anderson, J. B.: Distribution of glacial geomorphic features  
671 on the Antarctic continental shelf and correlation with substrate: implications for ice behaviour,  
672 J. Glaciol., 47, 397–411, 2001.

673 Wellner, J. S., Heroy, D. C., and Anderson, J. B.: The death mask of the antarctic ice sheet:  
674 Comparison of glacial geomorphic features across the continental shelf, Geomorphology, 75,  
675 157–171, <https://doi.org/10.1016/j.geomorph.2005.05.015>, 2006.

676 Weertman, J.: Stability of the junction of an ice sheet and an ice shelf, J. Glaciol., 13, 3–11, 1974.

677 Witus, A. E., Braneky, C. M., Anderson, J. B., Szczuciński, W., Schroeder, D. M., Blankenship, D. D.,  
678 and Jakobsson, M.: Meltwater intensive glacial retreat in polar environments and investigation  
679 of associated sediments: example from Pine Island Bay, West Antarctica, Quat. Sci. Rev., 85, 99–  
680 118, <https://doi.org/10.1016/j.quascirev.2013.11.021>, 2014.

681 Woodward, J., Smith, A. M., Ross,  
682 N., Thoma, M., Corr, H. F. J., King, E. C., King, M. A., Grosfeld, K., Tranter, M., and Siegert, M. J.:  
683 Location for direct access to subglacial Lake Ellsworth: An assessment of geophysical data and  
684 modelling, Geophys. Res. Lett., 37, L11501, doi:10.1029/2010GL042884, 2010.

685

686 **Figures**

687

688 Fig. 1. Multibeam bathymetry data over Anvers-Hugo Trough, Perrier Trough and Palmer Deep. Grid-  
689 cell size 30 m, displayed with shaded relief illumination from northeast. Regional bathymetry  
690 contours from IBCSO v1.0 (Arndt et al., 2013). Red dashed lines mark interpreted past grounding  
691 zone positions, with earliest ones labelled GZ1–GZ3. Most upstream grounding zone in Perrier  
692 Trough is labelled GZ3P, as it did not necessarily form synchronously with GZ3. Only discontinuous  
693 segments of later grounding zone positions are identified in Anvers-Hugo Trough. Black boxes show  
694 locations of Figs 2a and 5a. Red box on inset shows location of main figure.

695

696 Fig. 2. **a** Detail of multibeam bathymetry over the boundary of the mid-shelf basin in the southern  
697 part of Anvers-Hugo Trough. Grid-cell size 30 m, displayed with shaded relief illumination from 075°.   
698 Dashed red lines mark interpreted former grounding zone positions. Purple line marks location of  
699 MCS profile in Fig. 3, with small dots at intervals of 10 shots and larger dots and annotations at 100-  
700 shot intervals. White lines mark locations of topographic profiles in **b-d** and solid red lines mark  
701 locations of acoustic sub-bottom profiles in Fig. 4. Semi-transparent pink-filled areas crossing the  
702 sub-bottom profiles mark the positions of the buried channels observed in the profiles and  
703 interpolated between them. Yellow dotted line outlines approximate extent of area of anastomosing  
704 channels. MSGL, mega scale glacial lineations. **b** Profile across anastomosing channels. **c** Cross  
705 sections of northward shoaling valleys. **d** Profile along axis of one northward shoaling valley.  
706 Locations of profiles shown in **a**.

707

708 Fig. 3. Part of MCS Line AMG845-03 and interpreted line drawing, showing sedimentary basin pinch  
709 out at ~SP530. Dotted grey lines labelled B on the line drawing mark prominent bubble pulse  
710 reverberations following the sea-floor reflection. Location of profile, including shot point positions,  
711 shown in Fig. 2a.

712

713 Fig. 4. Acoustic sub-bottom (TOPAS) profiles from the southern part of Anvers-Hugo Trough showing  
714 buried, filled channels overlain by acoustically-transparent 'soft till' layer with MSGL on its surface,  
715 which is in turn overlain by a thin drape of postglacial sediments. Locations of profiles shown in Fig.  
716 2a.

717

718 Fig. 5. **a** Detail of multibeam bathymetry over the confluence between Anvers-Hugo Trough and  
719 Perrier Trough, which joins it from the east. Grid-cell size 30 m, displayed with shaded relief

720 illumination from northeast. Black lines marks locations of topographic profiles in **b-c**. Red line marks  
721 location of DTB profile in Fig. 6. Purple line marks location of MCS profile in Fig. 7, with small dots at  
722 intervals of 10 shots and larger dots and annotations at 100-shot intervals. Dark blue dashed lines  
723 outline selected box-shaped bathymetric basins. AHT, Anvers-Hugo Trough; MSGL, mega scale glacial  
724 lineations; GZ2, GZ3P, interpreted former grounding zone positions marked by dashed red lines.  
725 Orange dotted line marks lateral limit of MSGL, interpreted as position of palaeo-ice stream shear  
726 margins. **b** Cross sections of box-shaped basins running approximately SW-NE (i.e. approximately  
727 transverse to the inferred palaeo-ice flow direction). **c** Cross-section of one of the larger basins in an  
728 approximately NW-SE direction. Locations of profiles shown in **a**.

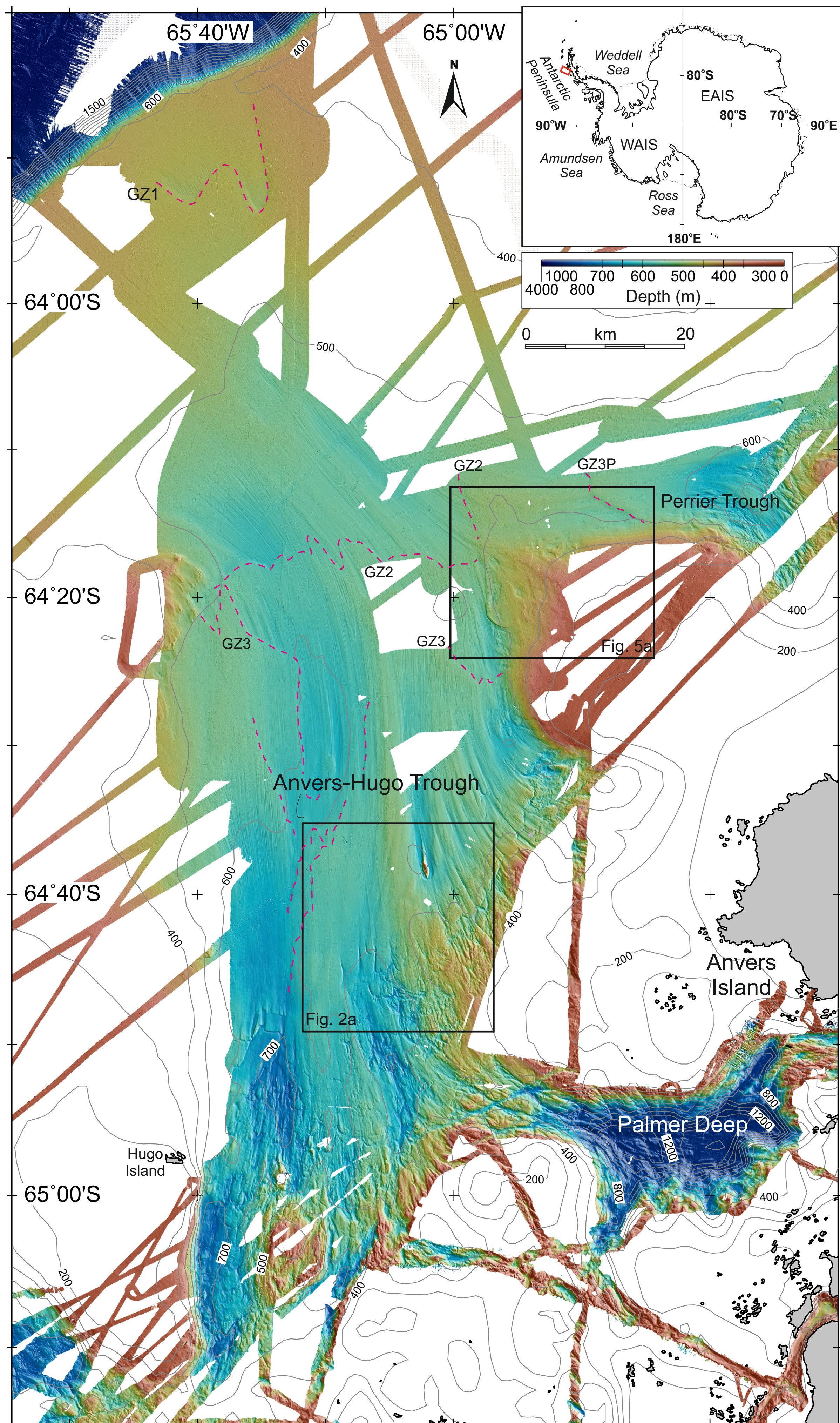
729

730 Fig. 6. Part of DTB Line 4 across the step-sided basin that lies closest to the trough confluence. The  
731 profile shows an acoustically-transparent layer of variably thickness, interpreted as Quaternary  
732 diamicton, overlying a strong reflector, interpreted as an unconformity above older sedimentary  
733 strata. Short segments of truncated, dipping reflectors, marked by upward pointing small arrows,  
734 can be seen beneath the strong reflector at the base of the acoustically-transparent layer. Two-way  
735 travel times have been corrected for the tow depth of the boomer so that they represent  
736 approximate times from the sea surface. Location of profile shown in Fig. 5a.

737

738 Fig. 7. Part of MCS Line BAS878-11 and interpreted line drawing, showing the entire area of the  
739 confluence between Anvers-Hugo Trough and a tributary trough is underlain by sedimentary strata,  
740 and that the lateral limit of MSGL in the tributary trough lies within 1 km of the position where a unit  
741 of younger strata with a distinct seismic facies character pinches out. An f-k demultiple process was  
742 used to suppress the sea-floor multiple reflection on this line. Dotted grey lines labelled B on the line  
743 drawing mark prominent bubble pulse reverberations following the sea-floor reflection. Location of  
744 profile shown in Fig. 5a.

745



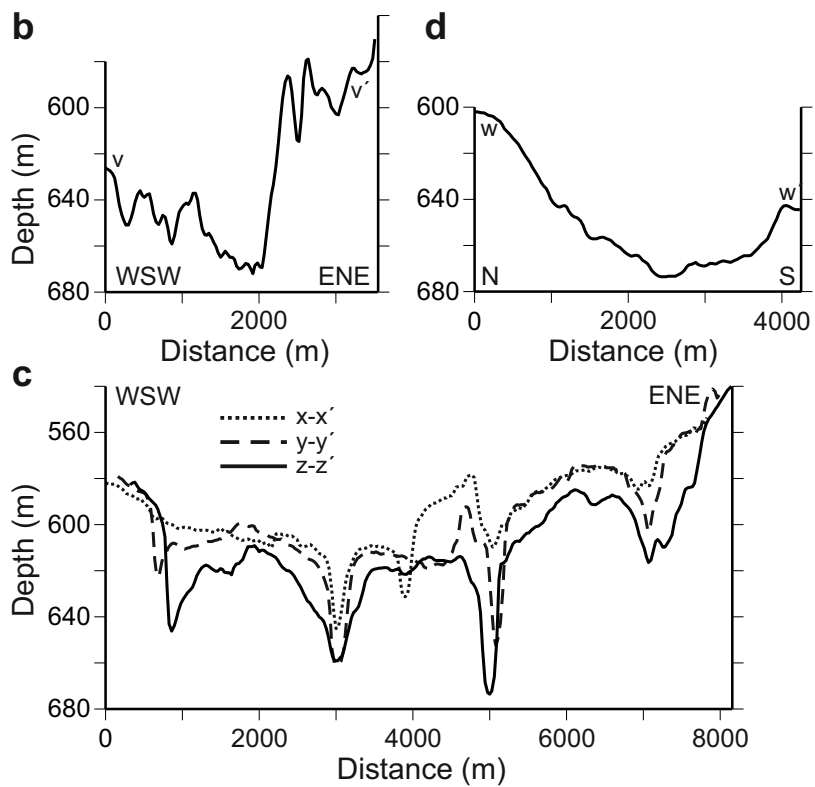
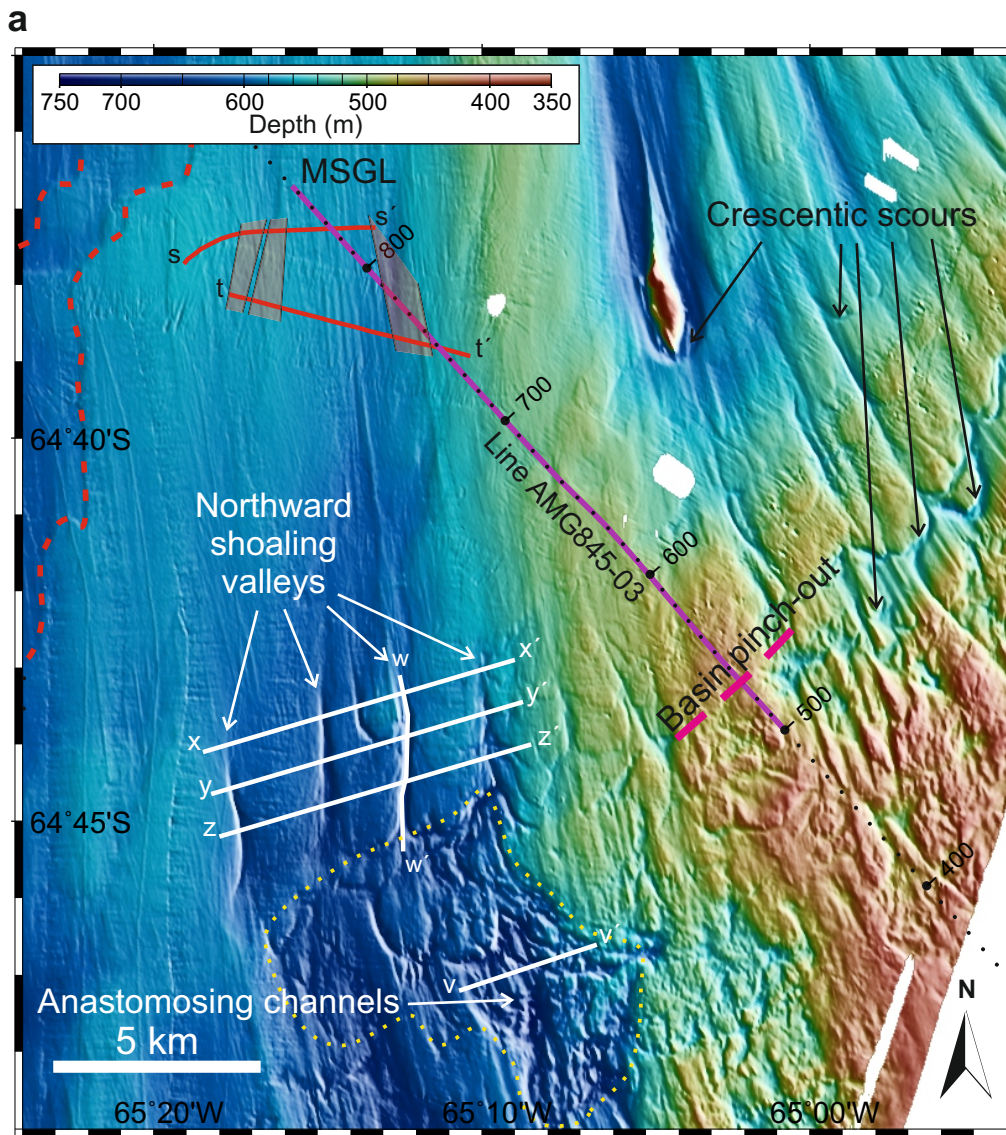


Fig. 2

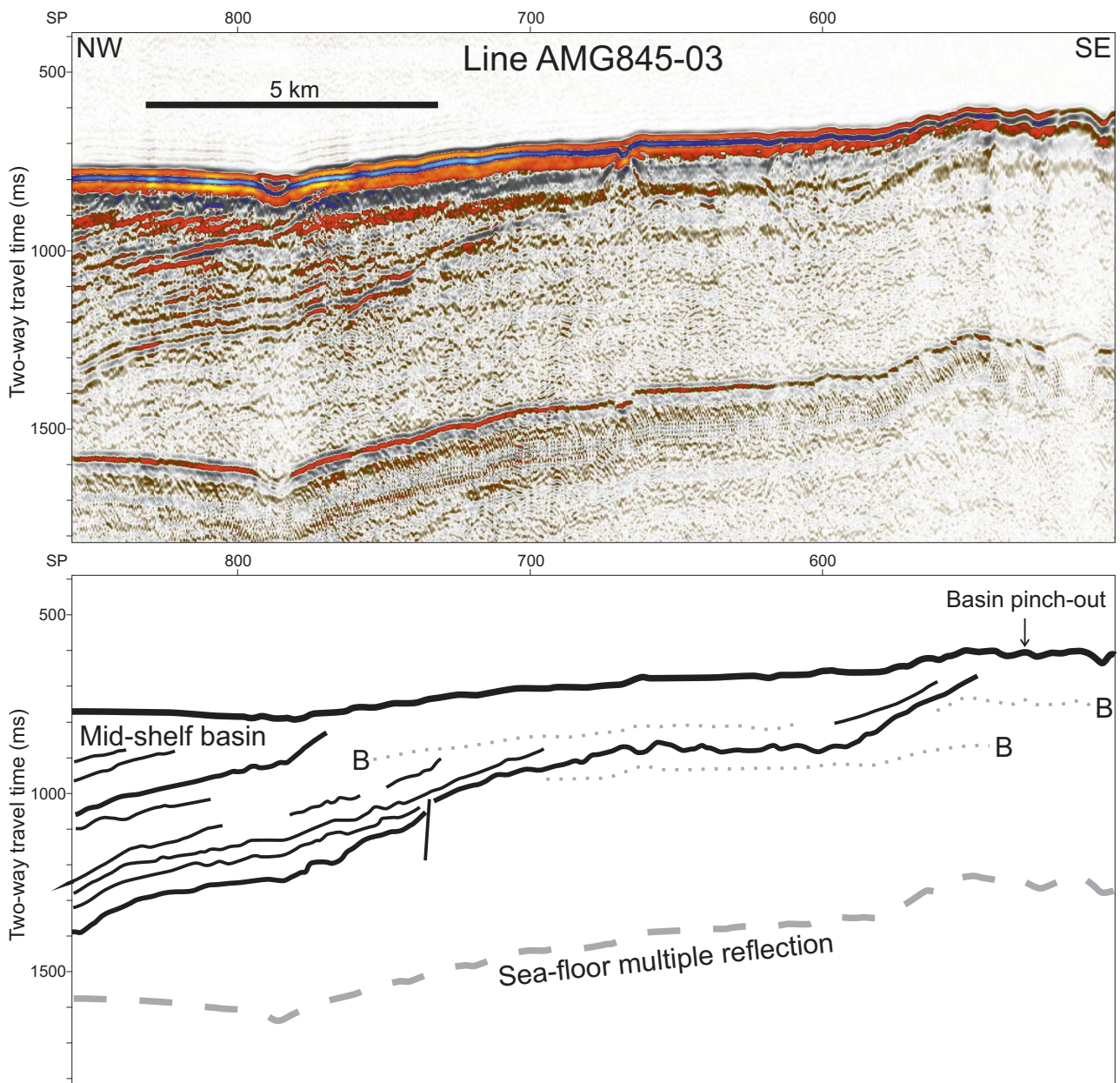


Fig. 3

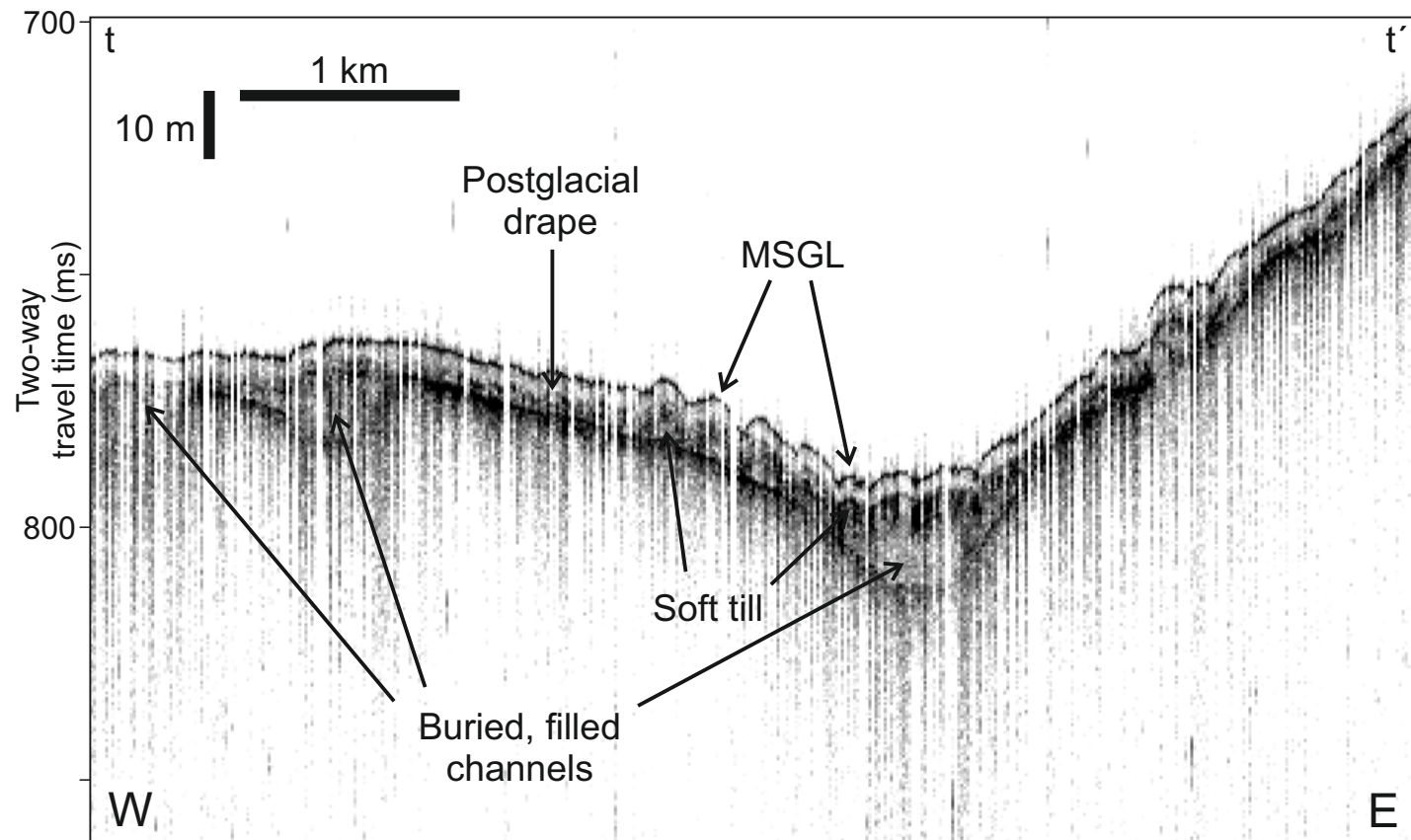
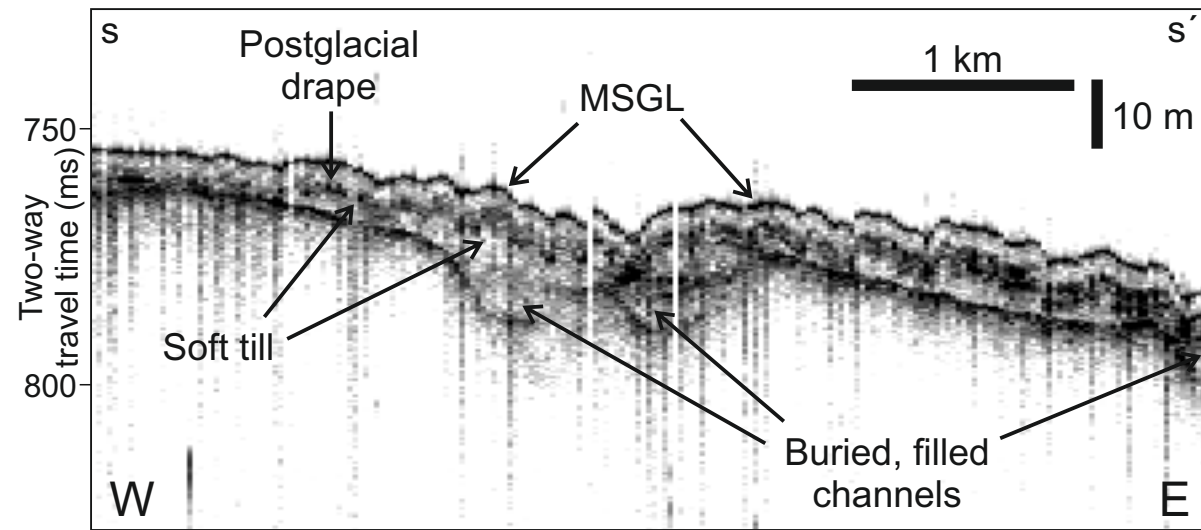


Fig. 4

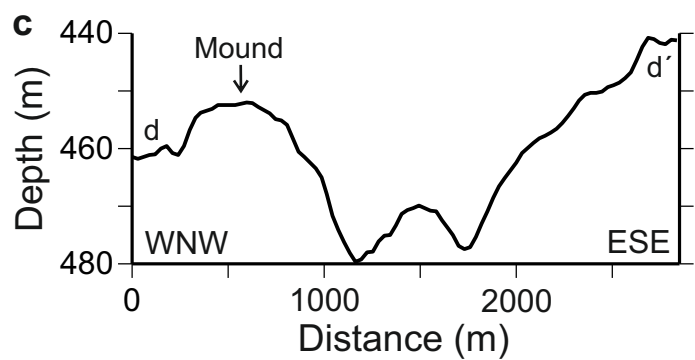
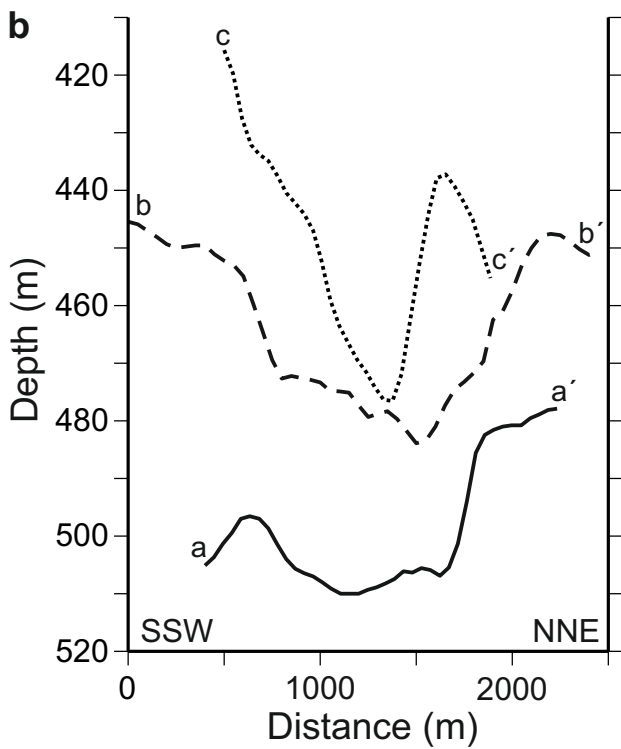
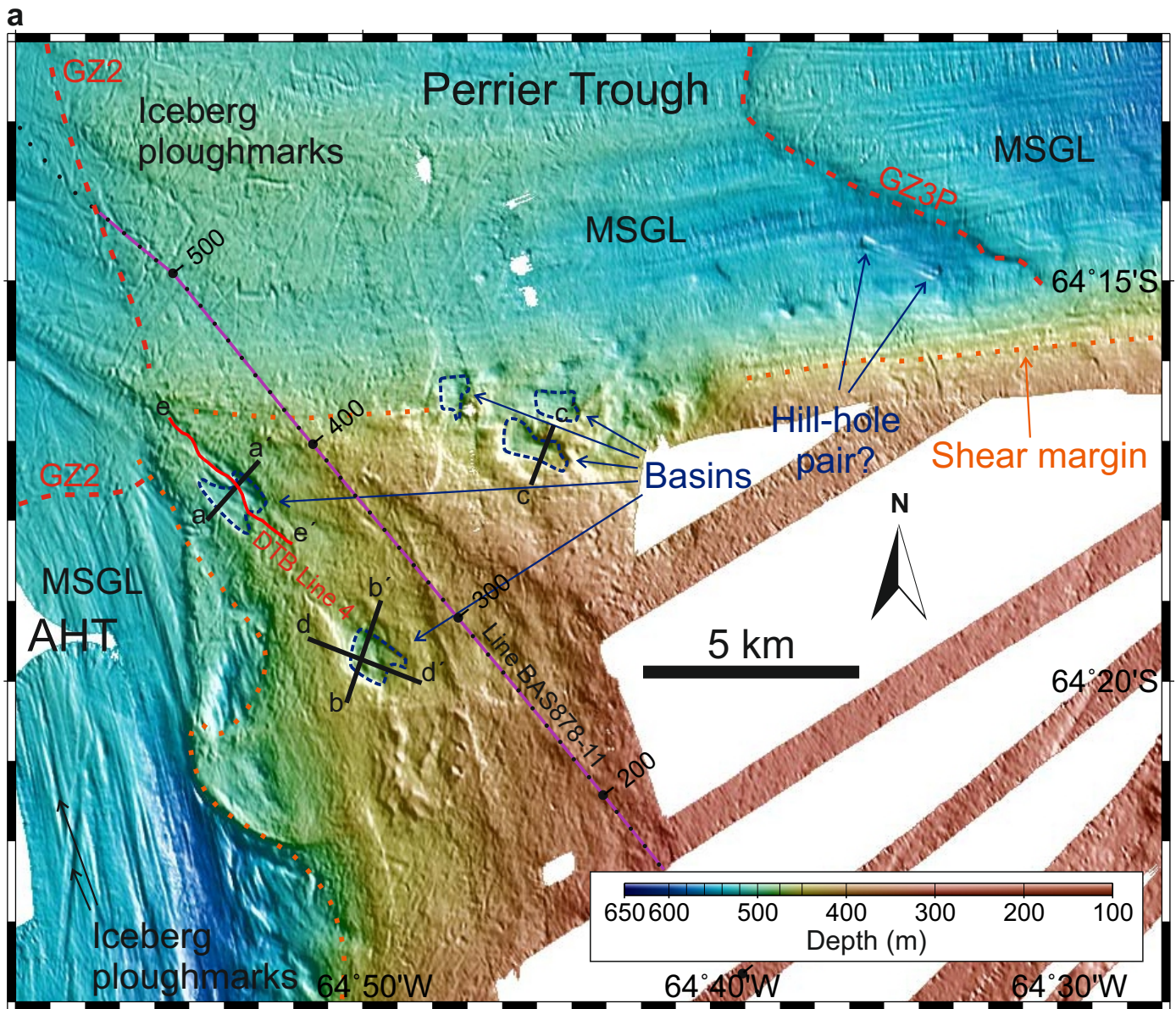


Fig. 5

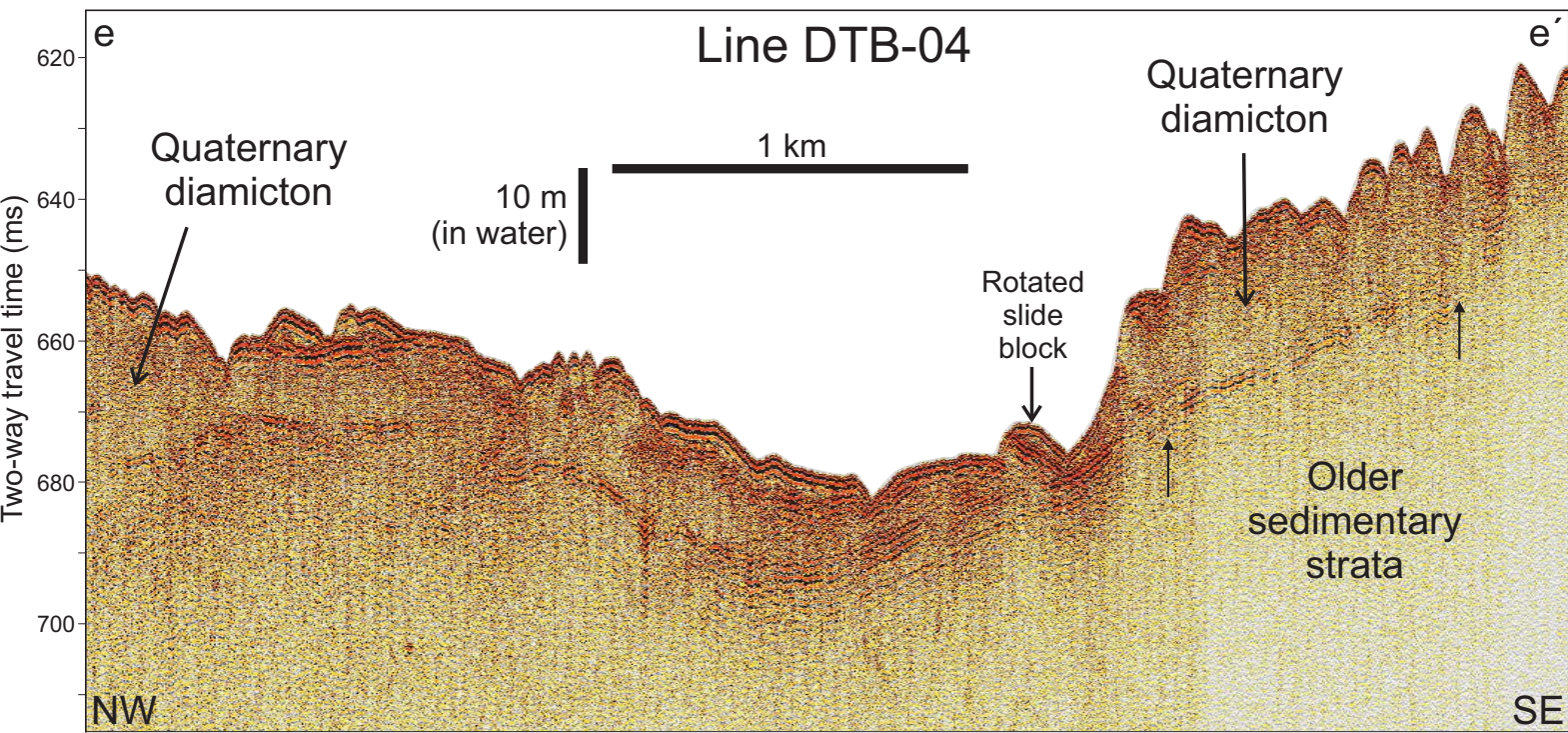


Fig. 6

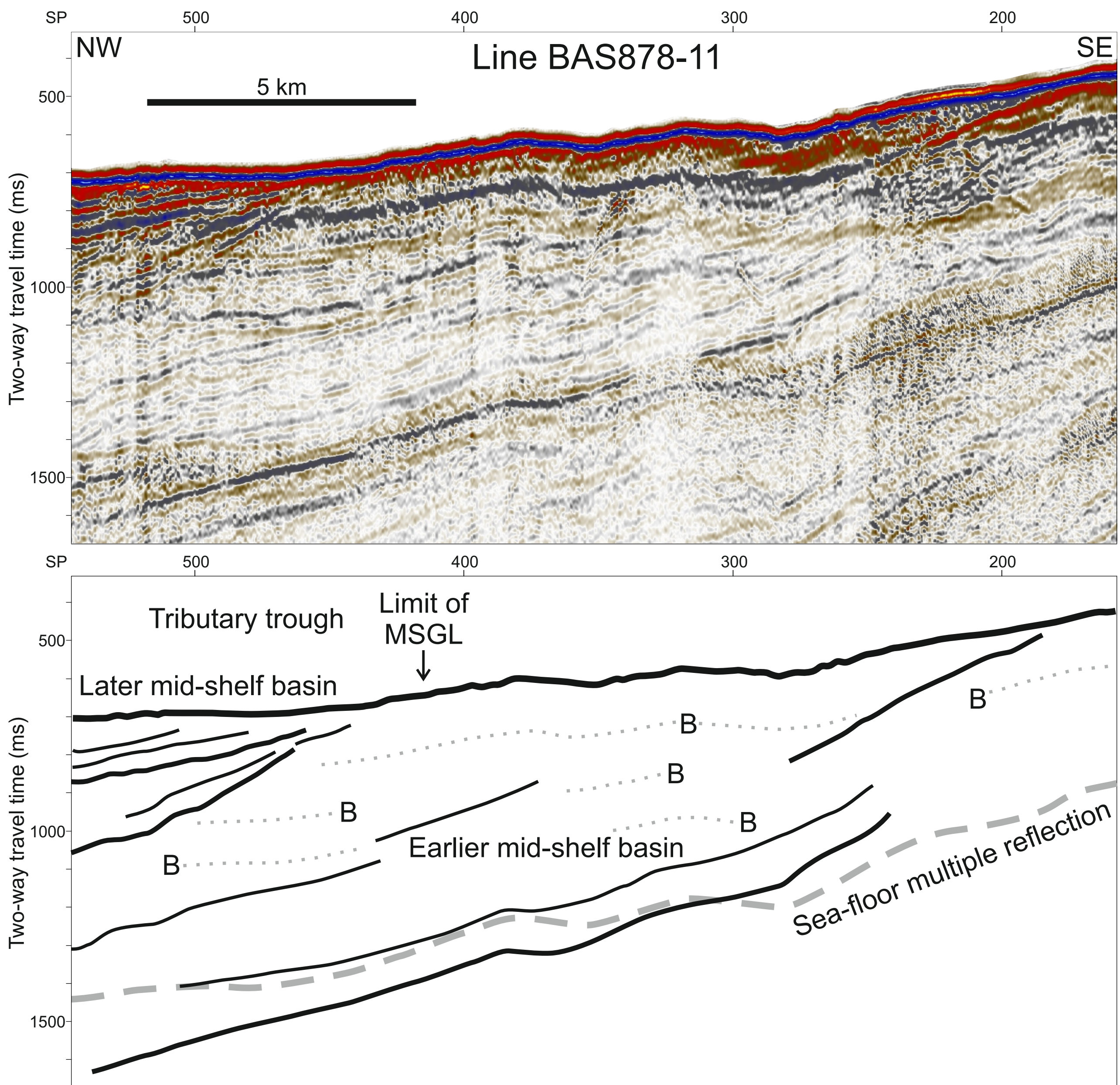


Fig. 7